EVALUATION OF THE RESIDUAL STRESSES IN A LOW TEMPERATURE CARBURIZED STAINLESS STEEL BY THE MICROHARDNESS MEASUREMENT

Giangiacomo Minak, giangiacomo.minak@unibo.it
Riccardo Panciroli, riccardo.panciroli2@unibo.it
Andrea Zucchelli, a.zucchelli@unibo.it
DIEM Alma Mater Studiorum – Università di Bologna viale del risorgimento 2, 40135 Bologna, Italia

Abstract.

Many attempts were made in recent years to engineer the surface of austenitic stainless steels to improve their hardness and tribological properties, without deteriorating their corrosion resistance, with the secondary effect of improving the fatigue properties of those materials.
Low temperature carburizing (LTC) treatment improves surface hardness and wear resistance of the austenitic stainless steels without reducing their corrosion resistance. Surface hardness over 1000 Vickers and compressive residual stresses whose modulus exceeds 1500 MPa are usually achieved in the carburized layer, having a thickness of some tens of microns, thanks to the formation of the so-called "S-phase", a carbon-supersaturated austenite phase.
Usually these quantities are measured independently by means of micro-hardness tests and X-ray diffraction, but since the mechanism that induces such high values of hardness and residual stresses is austenitic lattice expansion due to the carbon diffusion, without any other hardening mechanism, the micro-hardness increase should be a function of residual stresses only.
In this paper the results obtained by two numerical models developed by the Ansys code are shown.
The first model was used to calculate the residual stresses due to carbon supersaturation by means of a thermo-mechanical analogy, while the second to simulate the micro-hardness test on the material with the residual stresses field.
By joining the two methods it was possible to evaluate the distribution of the residual stresses with the final aim to take them into account for the fatigue life prediction of specimens and components.

Keywords: residual stress, low temperature carburizing, austenitic stainless steel, FEM, Vickers test

1. INTRODUCTION

Austenitic steels are widely used in the nuclear, chemical, food and pharmaceutical industries and in biomedical applications mainly because of their excellent corrosion resistance.
It is well know that these materials have good mechanical properties in terms of resistance and ductility, but a low hardness and consequently poor wear resistance.
A possibility of improving these properties is provided by different processes developed in the 1980's that consist in a low temperature carburizing, which involves the diffusion of large quantities of C atoms into the material at a diffusion temperature below 450 °C to prevent the formation of undesired chromium carbides and the degradation of the corrosion resistance.
In (Sun et al. 1999) the authors demonstrate that the phase produced by the nitriding, called the S-phase, has a highly distorted and disordered FCC austenitic structure, due to the formation of stacking faults and high compressive stresses. In the carbon S-phase, a high amount of carbon dissolved in the austenite causes the expansion and distortion of the FCC lattices of about 3% in the carburized layer, as in the nitrided layer.
The value of the micro hardness is quite high if compared with values obtainable by other treatments, and in the literature it ranges from 950 to 1200 HV (Ceschini & Minak, 2008, Stauder et al., 2003, Michal et al., 2006, Agarwal et al., 2007, Tokaij et al., 2004, Akita & Tokaij, 2006, Christiansen & Somers, 2006).
Such a hardness improvement, which is the primary goal of the LTC treatment, is mainly due to the residual stresses induced by the Carbon supersaturation.
Many authors have used X-Ray diffraction together with the layer removal technique to measure the biaxial residual stresses field in the LTC layer. Other conventional methods are not applicable due to the small size of the layer in which the residual stresses are present with a high stress gradient.
The values depend on the different carburizing process employed and range from a minimum of -1450 MPa, referenced in (Ceschini & Minak, 2008) to -1500 MPa found by Tokaij et al. (2004) and Akita & Tokaij (2006), -2000 MPa in (Michal et al., 2006 and Agarwal et al. 2007), up to -2400 MPa measured by Christiansen & Somers (2006). The depth involved by the compressive residual stress depends mainly on the treatment time (usually of the order of weeks) and is in the order of a few tens of microns.

These high values of compressive residual stresses and the consequent high value of surface hardness from one side reduce the wear rate (Ceschini et al. 2006) from the other affect the fatigue behavior.
The improvement of the resistance to fatigue loading is generally considered due to the retardation of crack nucleation provoked by the residual stresses and to the sub surface crack initiation. A survey of the experimental evidences on the fatigue behavior of LCT austenitic steels and on the general theories of the role of residual stresses (that are a particular case of stationary stress superimposed to the fatigue loading) can be found in Minak (2009).
Suresh and Giannkopoulos (1998) proposed a methodology for the determination of surface equi-biaxial residual stresses based on sharp (Vickers) indentation. The principle on which it is based is that a tensile residual stress would be expected to aid indentation by increasing the contact area for a given indentation load, while compressive residual stresses should act in the opposite way.
Bolzon et al. (2004) proposed a methodology that rests on the combination of experiments, computer simulation and inverse analysis to characterize the surface status and the material properties.
In that paper, geometrical data concerning the imprint generated in the specimen by the indentation test are considered an important experimental information, supplementary to the usual one consisting of measured indentation depth at various instants of the force cycle imposed on the indenter. Both kinds of data are employed as input in the subsequent inverse analysis for parameter identification. Information about the whole geometry of the residual imprint is exploited, not only the contact area like in (Suresh and Giannkopoulos 1998)
Aims of this paper are the numerical determination of the residual stress field in LTC austenitic steels from the knowledge of the distribution carbon content and the simulation of a Vickers test on a material in which the calculated stresses are present.
So, in the first part the stress distribution as a function of the point is found so that the actual stress field is considered in the zones in which the virtual micro-hardness test is performed.
Comparing the results of the simulated Vickers test with the experimental ones it was possible to measure indirectly, but in a cost-effective way, the residual stresses that can be used to foresee the fatigue life of these materials.

2. MATERIALS AND METHODS

The residual stress field and its measure by means of Vickers micro-hardness test in low temperature carburized austenitic stainless steels are studied. Since the source of residual stress is the austenitic lattice expansion the LTC process can be modeled considering the material as linear elastic. On the other hand the Vickers test is based on measure of the dimension of the imprint left by the indenter after unloading so in this phase the material is considered elasto-plastic with a bilinear law (for the sake of simplicity).
In the following sections, implementation and results of FEM analyses simulating the entire experimental procedure are presented and discussed. The ANSYS software was used for all the analyses. First, FEM was applied to analyze the residual stress field induced by the low temperature carburizing process, while a second model was developed to simulate a Vickers indentation on a narrow region of the specimen, characterized the residual stress field found in the first analysis.

2.1. Numerical determination of the residual stress field

A four-nodes PLANE182 element type was used in the analysis. A cylinder (15 mm height, 30 mm diameter) was modeled with an axisymmetric mesh, with progressively varying element size both from the axis to the lateral cylindrical surface as from the half-section to the upper and lower flat surfaces. The mesh has a total of 22000 elements and 22231 nodes. The carbon distribution curve through the thickness of the LTC specimen exhibits a typical diffusion profile with a maximum of about 10% on the surface gradually decreasing to zero in a few tens of microns towards the layer core interface (Stauder et al., 2003, Michal et al., 2006). To the LTC region is associated a volume increase proportional to the carbon content. For this reason, LTC process has been modeled by analogy with a thermal process: a thermal gradient having the same shape of the carbon content distribution (taken from Stauder et al., 2003 and Michal et al., 2006) and a maximum temperature increase ΔT=500 °C is applied. This way it is possible to simulate the volume expansion due to the carbon supersaturation by means of a thermal expansion, as proposed by Yang et al. (2005).
Even if during the LTC process all the external surfaces get carburized, the flat surfaces utilized for micrographic analysis and for hardness testing need to be polished and grounded before the Vickers indentation. Since these processes lead to the complete removal of the treated substrate, LTC is considered to be applied only to the cylindrical surface. The material was modeled as linear elastic with the following properties: Young's modulus E = 195GPa, Poisson's ratio ν = 0.3, and thermal expansion coefficient k=1.4e^{-5} °C^{-1}.
For a certain depth from the cylindrical surface, results are foreseen to be homogeneous all over the central part of the model, while border effect are expected close to the flat non-treated surfaces. Figure 1 shows the mesh refinement at the top-right corner of the cylinder section. The two lines represent the paths where the results are evaluated: line (1) lies on the flat surface (where the maximum of the border effect are foreseeable), while line (2) lies on a generic section far enough from the top surface to not be affected by any border effect.

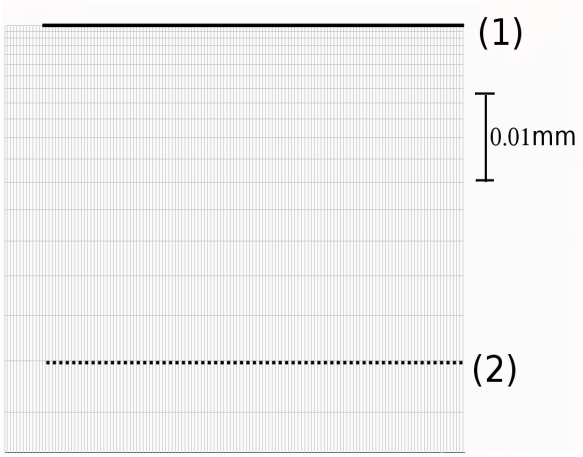

Figure 1: Detail of the mesh at the top-right corner of the cylinder section.

2.2. Simulation of the indentation process

In the Vickers test the contact area during indentation can be described as a square shape as shown in figure 2. For a certain indentation displacement, h, one can calculate the diagonal, d, by the following equation:

$$d = 2h\tan(136°)$$

The hardness is defined as the maximum applied load during the indentation test, P_{max}, divided by the residual contact area of the indentation A_s:

$$HV = \frac{P_{\max}}{A_s} = \frac{2\sin(136°)^2}{d^2} P_{\max} = 1.854\frac{P_{\max}}{d^2}$$

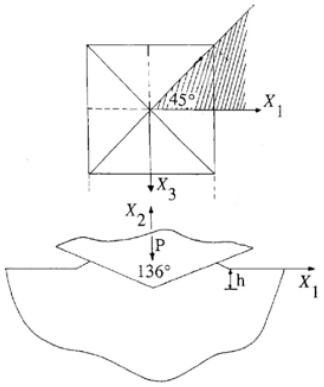

Figure 2: Scheme of the Vickers test

Two different models were developed to simulate a micro-hardness Vickers indentation test HV_{01} :

1) An axial-symmetric model was used to simulate the indentation on specimens with equal residual in-plane stresses ($\sigma_z=\sigma_\theta$, $\sigma_r=0$). A four-nodes PLANE182 element type was used in the analysis. As commonly done by other authors (Suresh and Giannakopoulos, 1998) the indenter was modeled as a rigid cone of half angle 70.3° in order to match the geometric characteristics of the Vickers pyramidal indenter. Prior to normal indentation, the substrate was equi-biaxially prestressed by means of the procedure described in the previous paragraph. The contact was modeled as frictionless. Depending on the initial prestress rate, 8 to 12 elements came in contact with the indenter. The total loading and unloading phase was applied in 30 unequal steps (smaller steps

are needed at the beginning of the contact to reach good convergence and accuracy of the elasto-plastic solution). Figure 3 shows geometry and discretization of the model.

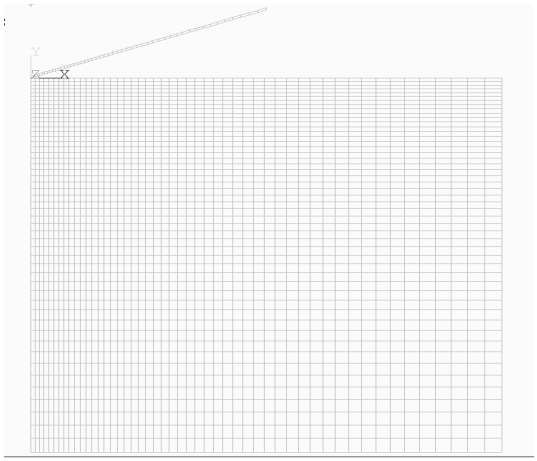

Figure 3: Two-dimensional axial-symmetric model

2) A second model was developed to simulate the Vickers indentation on specimens with unequal pre-existing residual stresses (σ_z=0, $\sigma_\theta \neq \sigma_r \neq 0$). Because of the non-axisymmetric residual stresses, a three-dimensional model was developed. An eight-nodes SOLID185 element type was used in the analysis. Even if it is possible to simplify the indenter geometry to an equivalent cone also in a three-dimensional simulation (Bocciarelli and Maier, 2007, Antunes et al., 2006) the real geometry of the Vickers indenter (modeled as a rigid body) is used in this case. Due to the symmetrical shape, only 1/8 of the model is considered. The contact is modeled as frictionless. Depending on the initial prestress rate, 6 to 8 elements came in contact with the indenter. Again, the total load was applied in 30 unequal steps.
Figure 4 shows geometry and discretization of the models.

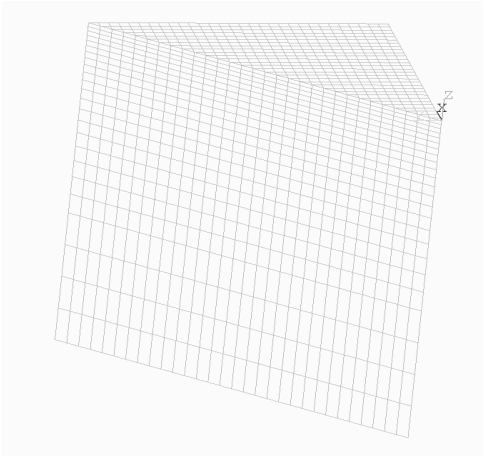

Figure 4: Three-dimensional model.

In both the analyses, the FE model dimensions were chosen in such a way that it is acceptable to assume that at the borders of the model the material remains linear elastic during indentation. The material was modeled with a bilinear elasto-plastic behavior with the following properties: Young's modulus E = 195GPa, Poisson's ratio ν = 0.3, yield strength σ_y = 360 MPa, plastic modulus E_y = 10GPa.

RESULTS

As a rule of thumb, the higher the carbon density, the more the lattice gets distorted, and the higher the residual stresses are expected. The numerically determined residual stress fields are shown in figures 5 and 6.

Figure 6, in particular, shows that in the central region, σ_z and σ_θ assume really close values and decrease with the same shape moving through the thickness, while σ_r is always close to zero. The residual stress is over at 45 μm depth. On the top (and bottom) flat surface, the stresses assume very different shapes: being on the surface, σ_z is clearly zero, while σ_r is not negligible anymore, representing the maximum component of the residual stress from a depth of 35 μm and below (figure 5).
The stress field obtained from these simulations will be used as reference for the Vickers indentation simulations on specimens with pre-existing residual stresses.

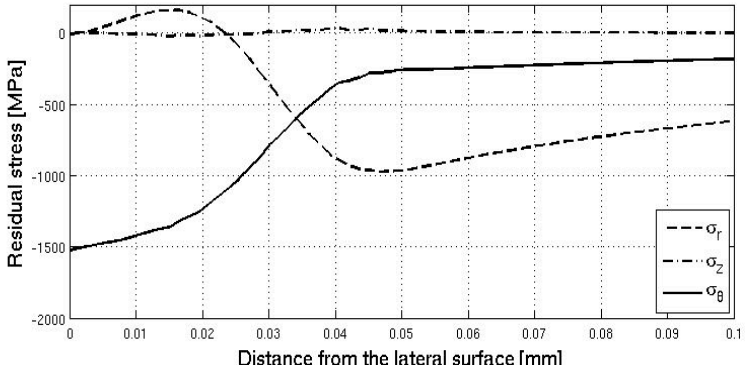

Figure 5: Residual stresses along path (1) of figure 1

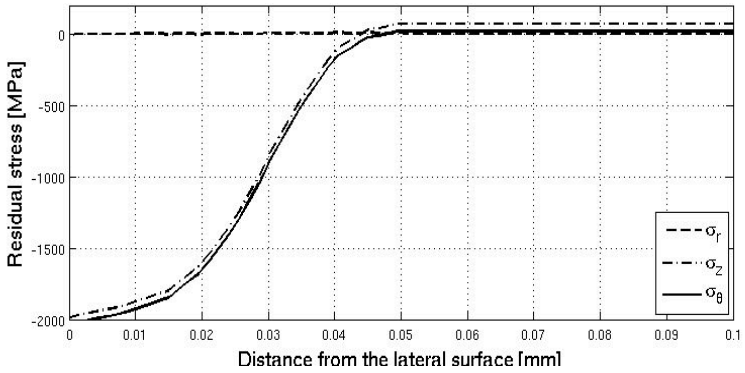

Figure 6: Residual stresses along path (2) of figure 1

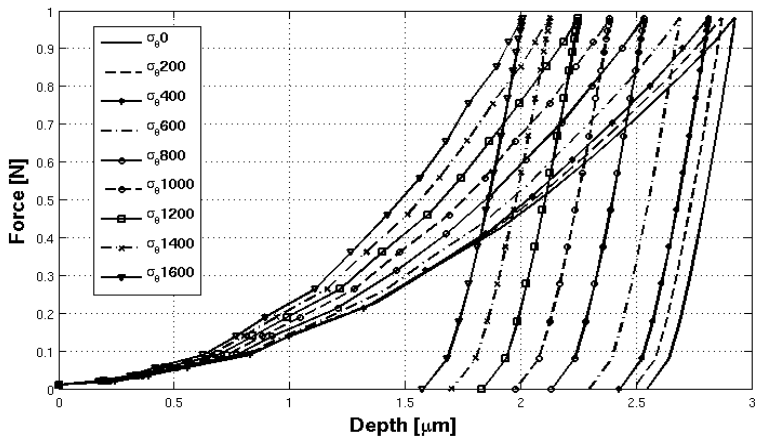

Figure 7: Numerical load-unload curves varying the pre-existing residual stress

Figure 7 shows a set of typical indentation force-depth curves varying the pre-existing residual stress. As expected, for a given indentation load the penetration depth is smaller in the presence of initial compressive self-stresses.

Figure 8 shows the predicted Vickers HV_{01} hardness in the case $\sigma_\theta=\sigma_z$, $\sigma_r=0$ varying the pre-existing residual stress, while the case $\sigma_r=\sigma_z=0$ is presented in figure 8. It has to be notice that: in the case only one stress component is present, the estimated hardness increases with the stress, while when there is more than one component, the estimated hardness shows an initial decrease, to later grow up.

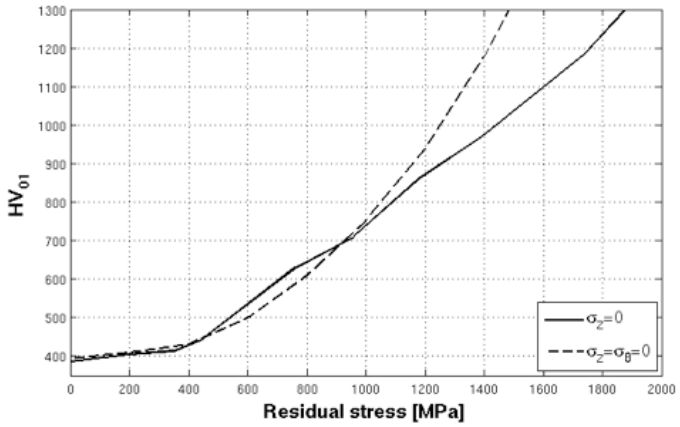

Figure 8: Predicted Vickers Hardness

Finally, applying the numerically evaluated pre-existing residual stress field (shown in figure 4) on the top flat surface, the Vickers hardness HV_{01} values can be evaluated numerically. Figure 9 shows a comparison between experimental data available in literature and the numerical results.
Even if the optima material parameters research (Bolzon et al. 2004) was not performed and typical values were used in the simulation, the agreement is quite satisfactory. It is worth noticing that the value of hardness corresponding to zero distance from the surface is commonly measured on the external surface that is in a different stress state (shown in figure 5).

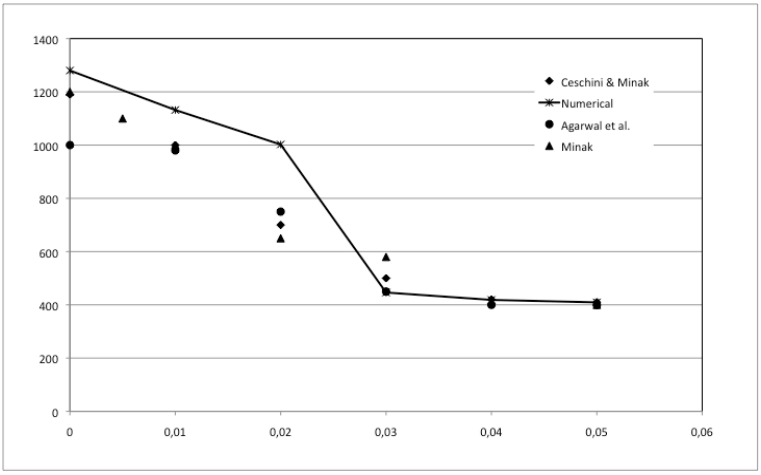

Figure 9: Predicted Vickers hardness along the carburized depth

3. CONCLUSION

In the present work two numerical methods were used to determine the residual stress field and the Vickers micro-hardness in low temperature carburized austenitic stainless steels from of the carbon concentration profile available in the literature.
The main results are the following: (i) the residual stress profile on a free surface is quite different from the one that is produced in the middle of the specimen; (ii) the simulation of the Vickers indentation process can take into account these both qualitative and quantitative differences; (iii) from the knowledge of the residual stress state in one point it is possible to derive the whole distribution; (iv) the Vickers micro-hardness test can be employed to determine the residual stress field as an alternative to x-ray diffraction in austenitic stainless steels.

4. ACKNOWLEDGEMENTS

The authors thanks Bodycote for funding the research and in particular Dr. Vittorio Bordiga

5. REFERENCES

Agarwal, N., Kahn, H., Avishai, A., Michal, G., Ernst, F., Heuer A.H., 2007, "Enhanced fatigue resistance in 316L austenitic stainless steel due to low-temperature paraequilibrium carburization", Acta Materialia, 55, pp 5572–5580

Akita, M., Tokaji, K., 2006, "Effect of carburizing on notch fatigue behaviour in AISI 316 austenitic stainless steel", Surface & Coatings Technology, 200, pp. 6073-6078

Antunes, J.M., Menes, L.F., Fernandes, J.V., 2006, "Three-dimensional numerical simulation of Vickers indentation tests", Int. J. of solids and structures, 43 pp 784-806

Bocciarelli, M, G. Maier, 2007, "Indentation and imprint mapping method for identification of residual stresses", Computational Material Science, 39 pp 381-392.

Bolzon, G., Maier, G., Panico, M., (2004), "Material model calibration by indentation, imprint mapping and inverse analysis", International Journal of Solids and Structures ,41 pp. 2957–2975

Ceschini, L., Minak, G., 2008, "Fatigue behaviour of low temperature carburized AISI 316L austenitic stainless steel" Surface & Coating Technology, 202, pp 1778–1784

Ceschini L., Lanzoni, E., Sambogna, G., Bordiga V., Schild T., (2006) "Tribological behaviour and corrosion resistance of Kolsterised austenitic stainless steel: existing applications in the automotive industry", Journal of ASTM International, 3(2), pp. 1 - 9

Christiansen, T., Somers, M.A.J, 2006, Characterisation of low temperature surface hardened stainless steel, Structure, 9, electronic format

Yang, Q., Ren, X., Gao, Y., Li, Y., Zhao, Y., Yao M., 2005, "Effect of carburzation on residual stress field of 20CrMnTi specimen and its numerical simulation", Materials science & Engineering A. 392, pp 240-247.

Michal, G.M., Ernst, F., Kahn, H., Cao, Y., Oba, F., Agarwal, N., Heuer, A.H., 2006, "Carbon supersaturation due to paraequilibrium carburization: Stainless steels with greatly improved mechanical properties", Acta Materialia, 54 pp 1597–1606

Minak, G., 2009 "On the improvement of the fatigue behaviour of austenitic stainless steels due to surface residual stresses", Proceedings of the 8th International Conference on Residual Stresses / 57th Denver X-ray Conference, in press.

Stauder, B., Jacquot, P., Prunel, G., Rey, O., Buvron, M., 2003," Influence de la cementation a basse temperature sur la resistance au grippage et a l'usure des aciers inoxydables austenitiques" Traitament Thermique, 349, pp 27-30

Suresh, S., Giannakopoulos, E., 1998, "A new method for estimating residual stresses by instrumented sharp indentation", Acta Materialia, 46 (16) pp. 5755-5767

Sun, Y., Li, X.Y., Bell, T., 1999, "X-ray diffraction characterisation of low temperature plasma nitrided austenitic stainless steels", J Mater Science, 34, pp 4793-4802

Tokaji, K., Kohyama, K., Akita, M., 2004, "Fatigue behaviour and fracture mechanism of a 316 stainless steel hardened by carburizing" International Journal of Fatigue, 26 pp. 543-551

6. RESPONSIBILITY NOTICE

The authors are the only responsible for the printed material included in this paper.